Rock Mech Rock Eng (2010) 43:667–676
DOI 10.1007/s00603-010-0101-x

ORIGINAL PAPER

Dynamic Characterization of Orthogneiss Rock Subjected to Intermediate and High Strain Rates in Tension

Ezio Cadoni

Received: 4 January 2010 / Accepted: 5 May 2010 / Published online: 22 May 2010

Abstract The dynamic characterization of rocks under intermediate and high strain rates is fundamental to understand the material behavior in case of heavy earthquakes and dynamic events. The implementation of material constitutive laws is of capital importance for the numerical simulation of the dynamic processes as those caused by earthquakes. These data are necessary and require experimental techniques able to induce on the rock materials state of loading reproducing the actual dynamic condition. The dynamic characterization has been carried out by means of two special apparatus: the split Hopkinson tension bar and the hydro-pneumatic machine. These equipments are briefly described with a discussion on the results of dynamic tension tests at three different strain rates (0.1, 10, 100 strain/s) on Onsernone Orthogneiss for loading directions 0°, 45° and 90° with respect to the schistosity. Results of the tests show a significant strain rate sensitive behavior, exhibiting dynamic tensile strength increasing with strain rate, up to about two times with respect to the quasi-static conditions in the case of 0° and 45° orientation and more than three times in the case of 90° at high strain rates. Dynamic increase factors versus strain rate curves for tensile strength were also evaluated and discussed.

Keywords Strain rate behavior · Dynamic tensile strength · Stress–strain curves · Intermediate loading rate · Dynamic increase factor

E. Cadoni (✉)
DynaMat Laboratory, University of Applied Sciences of Southern Switzerland, Via Trevano, P.O. Box 105-6952, Canobbio, Switzerland
e-mail: ezio.cadoni@supsi.ch

1 Introduction

The dynamic mechanical properties of rocks can be very different from those exhibited in quasi-static conditions. Specific investigations in such dynamic ranges appear necessary to correctly understand their behavior under intermediate and high strain rate conditions. Particular attention should be addressed to the dynamic tensile strength of rock materials that represent a relevant parameter to many rock mechanics applications.

The dynamic tensile strength can be obtained directly or indirectly by means of different experimental methods based on drop weight machines, split Hopkinson pressure bar (SHPB), gas gun, etc. The direct measurement of the dynamic tensile strength should be preferred because the measurement should be simple enough without introducing complexities such as a superposition of waves or inertia effects. Furthermore, rocks are often anisotropic in nature and their behavior is strongly influenced by anisotropy (Barla and Innaurato 1973).

In order to obtain the dynamic properties, the testing methods have to cover a wide spectrum of loading and strain rates. The strain rates achievable by the dynamic devices are typically from 10^{-1} to 10^{3} s^{-1}, while ordinary hydraulic testing machines can load specimens at strain rates up to 10^{-3} s^{-1}.

The interval where the dynamic devices operate can be divided in two main ranges as intermediate and high strain rates. The main performance of advanced techniques for high strain rate testing must be their capability of controlling and measuring wave propagation history as well as in the intermediate strain rate the inertial and vibration effects.

The strain rate obtainable by SHPB is on the order of 10^{0} to 10^{4} s^{-1}, but only indirect measurement of the tensile strength is available because it works in compression

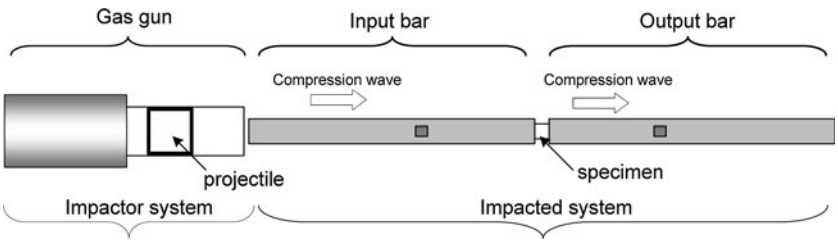

Fig. 1 Set-up of traditional split Hopkinson bar for compression tests

(splitting test, etc.). Some modification of the SHPB were used by different authors in order to obtain direct pulse (Zielinski 1982; Reinhardt et al. 1986; Albertini et al. 1996, 1997, 1999; Klepaczko and Brara 2001; Schuler et al. 2006, etc.).

Results from several research activities in rock mechanics are available in literature investigating influence of strain rate on mechanical properties of different types of rocks (i.e. Kubota et al. 2008). It is usually accepted that rocks exhibit higher strength values as strain rate increases; this behavior is mainly due to microscopic inhomogeneity, affecting principally sensitiveness to medium strain rates, and microcrack formations, failure surfaces development, which influence primarily high strain rates regime.

The direct measurement of the dynamic tensile strength of the Onsernone Gneiss (three strain rates for 0°, 45° and 90° orientations) has been carried out using the split Hopkinson tension bar (SPTB) and the hydro-pneumatic machine (HPM) installed in the DynaMat Laboratory of the University of Applied Sciences of Southern Switzerland.

2 Experimental Techniques at High and Intermediate Strain Rates

2.1 High Strain Rate Tests

The accuracy of the assessment of the rock mass subjected to dynamic loading strongly depends on the precision of the constitutive law in reproducing the real behavior of the rock materials. Particular attention needs to be addressed to the experimental results of high strain rates which have to be produced by means of devices able to measure the wave propagation in materials. The mechanical characterization of materials can be obtained in several modes (falling mass, gas gun, etc.), but the impact testing in tension and compression using the Hopkinson bar technique has shown distinct advantages and results (Cadoni et al. 2009). The most significant contribution of this method is that it avoids any filtering of signals, which could potentially cut out important information about the material behavior. As well known, the Hopkinson bar technique is widely used to determine the mechanical properties of structural materials under high strain rates; however, while the standard Hopkinson bar (with a diameter in the range of 10–20 mm) is sufficient for dynamic testing of fine-grained materials (i.e. Carrara marble), larger bars are needed to load representative volumes of heterogeneous rocks (Albertini et al. 1996, 1997, 1999).

2.1.1 The Traditional SHPB

The traditional SHPB, shown in Fig. 1, works mainly in compression and consists principally in a projectile generating an impact loading pulse by impinging on an input bar which transmits the load to the specimen sandwiched between input and output bar.

When the incident pulse reaches the specimen, part of it is reflected by the specimen whereas another part passes through the specimen propagating into the output bar. Strain-gauges glued on the input and output bars of the SHPB are used for the measurement of the elastic deformation (as a function of time) created on both half-bars by the incident (ε_I)/reflected (ε_R) and transmitted (ε_T) pulses, respectively.

The application of the elastic uniaxial stress wave propagation theory of the Hopkinson bar system (Davies 1948; Kolsky 1949) allows to calculate the forces F_1 and F_2 and the displacements δ_1 and δ_2 acting on the two faces of the specimen in contact with the input and output bars, respectively, by means of the following relationships, which are based on the recorded strains ε_I, ε_R, ε_T of the elastic input and output bars:

$$F_1 = E_0 A_0 (\varepsilon_I + \varepsilon_R) \tag{1}$$

$$F_2 = E_0 A_0 \varepsilon_T \tag{2}$$

$$\delta_1 = C_0 \int (\varepsilon_I - \varepsilon_R)\, dt \tag{3}$$

$$\delta_2 = C_0 \int \varepsilon_T\, dt \tag{4}$$

where E_0 is the bar elastic modulus, A_0 the bar cross-section area, and C_0 is the elastic wave velocity.

Under a homogeneous stress state, the stress and the strain of the material can be determined with the following relationships:

$$\sigma = \frac{F_1 + F_2}{2A_s} \tag{5}$$

$$\varepsilon = \frac{\delta_1 - \delta_2}{L_s} \tag{6}$$

$$\dot{\varepsilon} = \frac{d\varepsilon}{dt} \tag{7}$$

where L_s is the specimen length, A_s the specimen cross-sectional area, and t is the time.

When the specimen is short, so that the travel time of the wave through the specimen is small in comparison to the duration of the test, the specimen can be considered as being in load equilibrium at its ends, and in homogeneous stress state created by the many wave reflections taking place at the ends (interfaces specimen bars) of the specimen. These last experimental conditions constitute the basic assumptions in order to calculate the average stress–strain characteristics of the specimen material at different strain rates, through the following equations:

$$\sigma(t) = E_0 \frac{A_0}{A_s} \varepsilon_T(t) \tag{8}$$

$$\varepsilon(t) = -\frac{2C_0}{L_s} \int_0^t \varepsilon_R(t)\, dt \tag{9}$$

$$\dot{\varepsilon}(t) = -\frac{2C_0}{L_s} \varepsilon_R(t) \tag{10}$$

2.1.2 *The JRC-Split Hopkinson Tensile Bar (JRC-SHTB)*

The SHTBs installed in the DynaMat Laboratory of the University of Applied Sciences of Southern Switzerland have been developed during the last three decades by the researcher of the Joint Research Centre of the European Commission (Albertini and Montagnani 1974; Cadoni et al. 1997). This innovative modification of the Hopkinson bar version is capable of performing impact precision tests in tension, compression, bending and shear using the same loading device and the same measuring equipment and instrumentation. The main modification introduced into the traditional split Hopkinson bar consists in the substitution of the projectile, normally used to generate the impact loading pulse, with a statically pre-stressed bar which is the physical continuation of the input bar.

The JRC-SHTB used for rocks characterization consists in two circular aluminum bars, called input and output bars, having a length of 3 and 6 m, respectively, with a diameter of 20 mm to which the specimen is glued on using a bi-component epoxy resin. The input bar is connected with a high strength steel pretension bar 6 m in length, used as pulse generator with a diameter of 12 mm in order to obtain the same acoustical impedance of the input bar so that the pulse reflection, due to the interface, is avoided.

A test with the JRC-SHTB is performed as follows:

Fig. 2 DynaMat Laboratory: set-up for the high strain rate tensile tests on specimen Ø = 20 mm

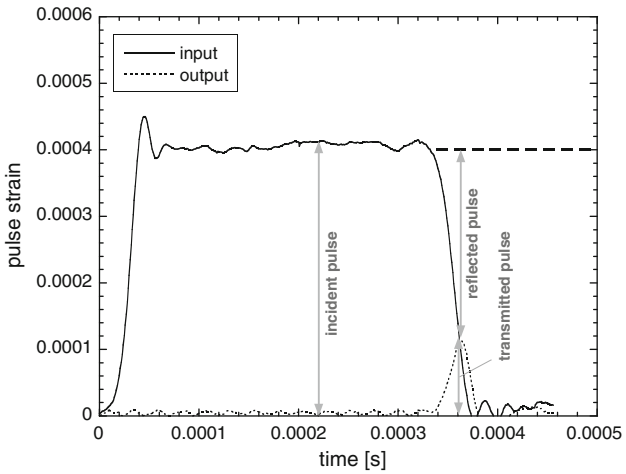

Fig. 3 Signals measured on the input and output bars versus time curves of gneiss rock

(a) First, a hydraulic actuator, of maximum loading capacity of 600 kN, is pulling the pretension high strength steel bar; the pretension stored in this bar is resisted by the blocking device (see Fig. 2).
(b) Second, operation is the rupture of the fragile bolt in the blocking device which gives rise to a tensile mechanical pulse of 2.4 ms duration with linear loading rate during the rise time, propagating along the input and output bars bringing to fracture the specimen.

The pulse propagates along the input bar with the velocity C_0 of the elastic wave with its shape remaining constant. When the incident pulse (ε_I) reaches the rock specimen, part of it (ε_R) is reflected by the specimen whereas another part (ε_T) passes through the specimen propagating into the output bar as shown in Fig. 3. The

relative amplitudes of the incident, reflected and transmitted pulses, depend on the mechanical properties of the specimen. Strain-gauges glued on the input and output bars of the device are used for the measurement of the elastic deformation (as a function of time) created on both half-bars, respectively, by the incident/reflected and transmitted pulses.

This modified system still satisfies the condition of applicability of the uniaxial elastic wave propagation theory because the pulse wavelength (in order of a few meters) is much higher than the transverse length of the bar (20 mm).

The main advantage of the JRC-SHTB with respect to the traditional one lies mainly in the fact that the generation of the loading stress pulse is performed by means of a statically pre-stressed bar which is the physical continuation of the input bar, therefore avoiding the difficulties connected to the launching and impacting of projectiles. This characteristic has allowed the generation of very long loading pulses. A pulse of 40 ms duration obtained by 100 m (Albertini et al. 1999; Cadoni et al. 1997, 2000, 2001a, b, c) length of pre-stressed bar is a feature unimaginable with the projectile impactor technique (it would have been necessary to launch a 100 m length projectile). Such long duration loading pulses are required for testing very ductile materials and structural components.

Also the impact testing with the impacting projectile of the classical Hopkinson bar requires perfect alignment and plane impinging of the projectile on the input bar, which are very demanding conditions for engineering testing. In contrast, in the modified Hopkinson bar, the loading pulse passes smoothly and plane from the pre-stressed bar to the input bar because one is the physical continuation of the other.

The JRC-SHTB equipment can be considered as a transducer system which allows the measurement of the load–displacement characteristic of the specimen by exerting strict control over stress wave propagation. The JRC-SHTB permits to perform dynamic tension tests at high strain rates that are very difficult to conduct for rocks. The measurement of the tensile strength of rocks is usually obtained by the utilization of the SHPB with the Brazilian or splitting test set-up (Wang et al. 2009; Tedesco et al. 1993, etc.). The difficulties of the direct tests have often discouraged and impeded the development of such set-up. The relevant results obtained with concrete material have clearly demonstrated the potentiality of SHTB for the dynamic characterization of brittle materials such as rocks.

2.2 Intermediate Strain Rate Tests

The intermediate strain rate tests have been carried out by means of a HPM.

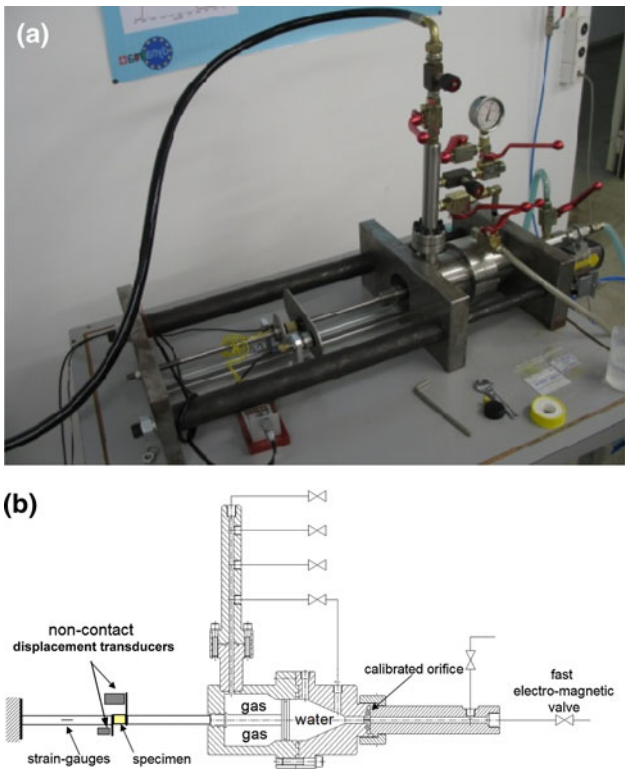

Fig. 4 Hydro-pneumatic machine used for intermediate strain rate tests

The employed HPM is shown in Fig. 4a and b. At the beginning of the test, a sealed piston divides a cylindrical tank in two chambers: one chamber is filled with gas at high pressure (e.g. 150 bar), the other one is filled with water. At the beginning, equal pressure is established in the water and gas chambers so that the forces acting on the two piston faces are in equilibrium. The test starts when the second chamber discharges the water through a calibrated orifice, activated by a fast electro-valve. Then, the piston starts moving expelling out the gas through a sealed opening; the end of the piston shaft is connected to the steel specimen; the specimen is linked to the piston shaft and to one end of an elastic bar, whose other end is rigidly fixed to a supporting structure. When the piston shaft moves, the specimen is pulled at a fixed strain rate level, depending on the velocity of the gas expelling from the chamber. The elastic bar is instrumented with a strain-gauge that provides, through the elastic properties of the bar, the force acting on the specimen during the test. Two targets are attached on both ends of the specimen and their movements are measured by two contact-less displacement transducers.

It can be evidenced that a constant speed movement of the piston guarantees the constancy of the strain rate during the test; this depends mainly on the constancy of the force exerted by the gas pressure on the piston face. A good result in this sense was obtained with a small change of gas

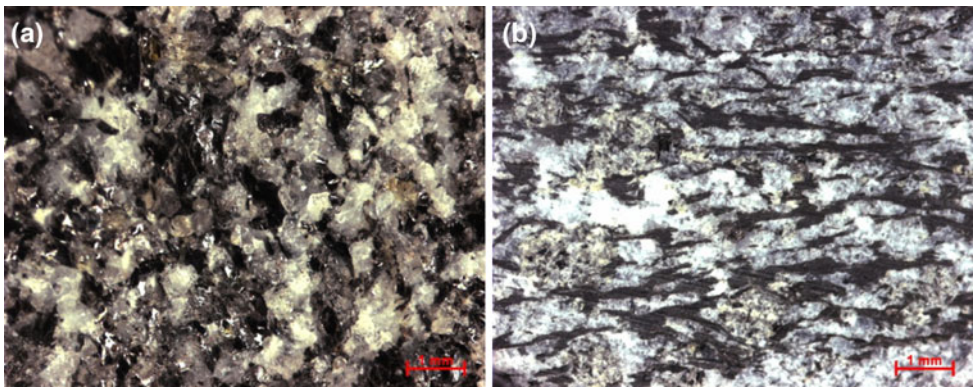

Fig. 5 **a** The microcrystalline structure of the Onsernone Gneiss; **b** the schistosity

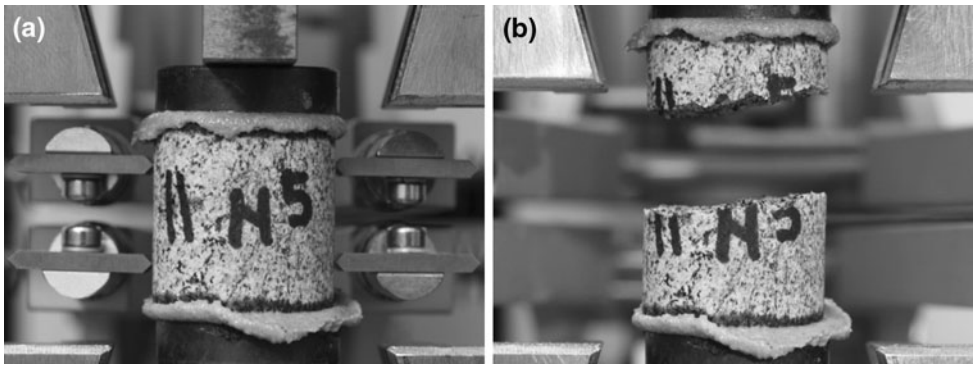

Fig. 6 Static test before (**a**) and after failure (**b**) of the Onsernone Gneiss

volume during the test in order to have small gas pressure decrease and consequently small piston force decrease. Furthermore, the load P resisted by the specimen is measured by the dynamometric elastic bar, whereas the specimen elongation ΔL is measured by the displacement transducers, sensing the displacement of the plates target fixed to both specimen ends. Such acquisitions allow to obtain the stress versus strain relationship at the strain rate level, achieved during the test.

3 Materials

The rock material used for testing is an Orthogneiss from the Onsernone Valley (Swiss Alps) of the Cantone Ticino (Switzerland). Its petrography is characterized by the presence of white feldspar (albite) and transparent quartz. Also included are a relatively large quantity of white mica (muscovite) and dark mica (biotite) even if this is not evenly distributed (see Fig. 5a, b). The mean grain size of the crystals is about 0.5 mm while the maximum grain size is 1 mm (see Fig. 5a).

Series of cores (diameter = 20 mm, height/diameter = 1) was drilled out in three directions: the first parallel ($\theta = 0°$) and the second perpendicular ($\theta = 90°$) to the plane of schistosity, the third sampling direction oriented at $\theta = 45°$ to the plane of schistosity. As result θ is then defined as the angle of schistosity with the loading direction.

The material is characterized by an apparent density of 2,710 kg/m^3 and an absolute density of 2,740 kg/m^3. The Young's modulus at $\theta = 0°$ is 39.3 GPa and its Poisson's ratio is 0.3. The compression strength has been evaluated on three samples for each θ and the mean values are 189 ± 8 and 203 ± 7 MPa for $\theta = 0°$ and $\theta = 90°$, respectively. In order to compare dynamic and quasi-static regime directly, excluding the results of any size effect influence, the tensile static strength has been measured on 20 mm diameter, 20 mm high specimens (the same geometry of the dynamic tests). Three specimens have been used to evaluate the tensile strength for each θ and the mean values are 12.6 ± 0.5, 6.1 ± 0.8 and 2.6 ± 1.1 MPa for $\theta = 0°$, $\theta = 45°$ and $\theta = 90°$, respectively. Figure 6 shows a specimen in static test, before and after failure.

4 Tensile Test Results

4.1 High Strain Rate tests

The results of the tests at high strain rates carried out with the SPTB equipment are shown in Table 1. The tests have been performed in tension with the load in three orientations $\theta = 0°$, $\theta = 45°$ and $\theta = 90°$ with respect to the

Table 1 High strain rate results

ID	Orientation of schistosity (°)	Dynamic tensile stress, $f_{t,d}$ (MPa)	Mean value, f_{t,d_ave} (MPa)	Fracture energy, $G_{f,d}$ (J/m^2)	Mean value, G_{f,d_ave} (MPa)	Stress rate, $\dot{\sigma}$ (GPa/s)
0_N1	0	25.71	25.45 ± 0.4	1,260	1,304 ± 183	1,161
0_N2	0	24.96		1,146		1,151
0_N6	0	25.70		1,505		870
45_N3	45	8.07	13.52 ± 4.7	414	868 ± 397	405
45_N4	45	16.86		1,154		788
45_N7	45	15.65		1,036		737
90_N1	90	6.50	8.67 ± 1.89	691	712 ± 81	257
90_N4	90	9.56		801		545
90_N6	90	9.96		643		534

schistosity plane. The strain rate of the test is dependent on two variables: the behavior of the material and the loading of the pre-stressed bar. A constancy of the pre-load has been chosen in order to verify the response of the rock specimen under the same loading condition (in this case a preload of 18 kN) varying the orientation schistosity.

The measurements of the strain histories of the input and output bars were used for the determination of the stress versus strain curves by Eqs. 8 and 9. In Fig. 7, the stress versus strain curves for the three orientations are shown. These diagrams confirm that the SHTB is able to measure both the ascending and descending branch of the curve and permits to measure the fracture energy (computed as the subtended area in a stress–crack opening displacement curve). The value of the fracture energy at a high strain rate depends on the orientation of schistosity. Higher values can be observed for the $\theta = 0°$, while lower values are for $\theta = 90°$, then fracture energy reveals an increasing trend with the orientation.

This increase in fracture energy shows that at $\theta = 0°$ this Orthogneiss is more ductile. In order to understand better the ductility and/or brittleness of this material, the characteristic length (Hillerborg et al. 1976) should be considered. As a unique material property, the characteristic length $l_{ch} = G_F E/f_t^2$ expresses fracture of concrete-like materials, where the l_{ch} is proportional to the square of the tensile strength. This means that brittleness decreases with high fracture energy and increases with an increase in strength of material. The values at $\theta = 0°$, $\theta = 45°$ and $\theta = 90°$ are 79, 192 and 413 mm, respectively. The lower value is for $\theta = 0°$ revealing less brittle behavior with respect to the other two ($\theta = 90°$ and $\theta = 45°$). The brittleness increases also with the strain rate (Asprone et al. 2009).

The stress rate caused by the incident pulse has been maintained constant by the preload condition, and it is about 1,150 GPa/s. By measuring the slope of the stress versus time curves, the stress rate for each test can be obtained. The results are reported in the last column of Table 1. In SHTB device, the different stress rates are caused by different preloads of the pretension bar.

Varying θ, the specimen failure can be influenced by the preferential plane of fracture. In the case of $\theta = 0°$, the fractures obtained are orthogonal to the loading direction (see Fig. 8a) and the repeatability of the tests is very good as shown in Table 1 (low standard deviation). In the case of $\theta = 45°$ and $\theta = 90°$, particular failures might occur. In Fig. 8b and c, two typical fractures in the case of $\theta = 45°$ are shown (the second one (45_N3) with the low strength).

4.2 Intermediate Strain Rate tests

The intermediate strain rate tests have been carried out using a HPM with two different calibrated orifices with diameters of 1 and 3 mm. With the lower diameter, the intermediate velocity (about 200 MPa/s) is lower than the one obtained (about 1,500 MPa/s) with the greater diameter. The results are shown in Table 2. The tests have been carried out in tension for $\theta = 0°$, $\theta = 45°$ and $\theta = 90°$.

5 Strain Rate Effect

The dynamic effect on the tensile strength can be represented by the ratio between the dynamic and static strength, well known as dynamic increase factor (DIF $= f_{t,dynamic}/f_{t,static}$). Several researchers have found out that DIF of strength increases with strain rates. This ratio is usually higher for low strength rocks, and lower for high strength rocks. For example, the DIF for yellow tuff (Asprone et al. 2009) is about 3 using direct dynamic tension test (SHTB), and for high strength rocks (Dutta and Kim 1983) the DIF is about 2 using the Brazilian test by means of the SHPB.

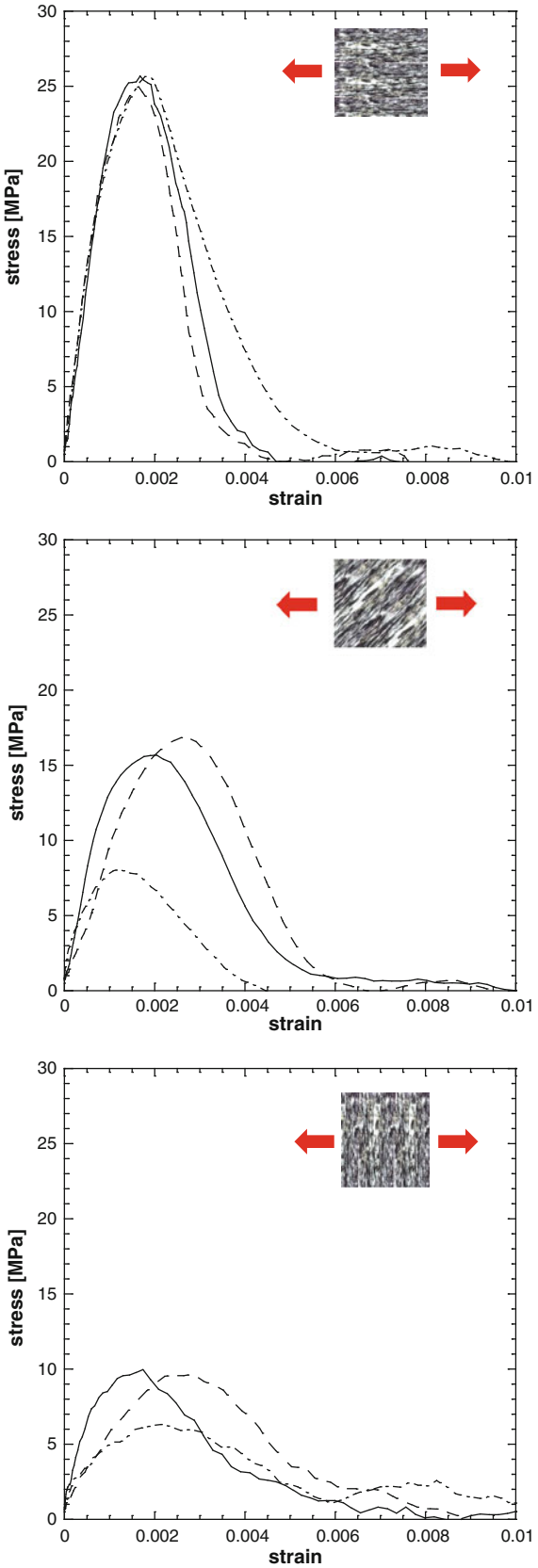

Fig. 7 Dynamic stress versus strain curves of Orthogneiss in tension for $\theta = 0°$, $\theta = 45°$ and $\theta = 90°$

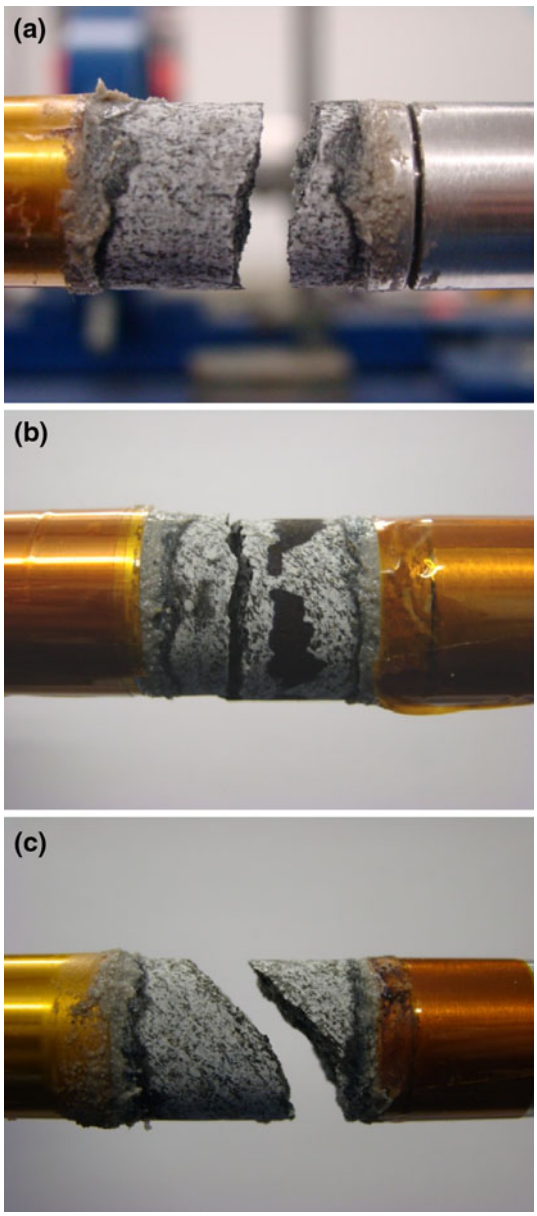

Fig. 8 Specimen after SHTB tests: **a** $\theta = 0°$, **b**, **c** $\theta = 45°$

DIF has been extensively used in order to quantify strain rate effects for concrete-like materials in a large number of experimental researches. From these results, some expressions of the DIF on the tensile strength have been developed but unfortunately these do not consider any corrections taking into consideration the type of materials (grain size, aggregate type and maximum size, specimen size, water content, etc.) neither the type of experimental set-up used to determine the dynamic tensile strength. As reference, three of them are here recalled as:

(a) the DIF formula proposed by the Comité Euro-International du Béton (1993) for concrete in tension with strain rates up to 300 s^{-1}:

Table 2 Intermediate strain rate results

ID	Orientation of schistosity (°)	Dynamic tensile stress, $f_{t,d}$ (MPa)	Mean value, f_{t,d_ave} (MPa)	Stress rate, $\dot{\sigma}$ (GPa/s)
0_N3	0	19.78	17.39 ± 2.4	1.752
0_N4	0	17.56		1.370
0_N7	0	14.82		1.439
0_N8	0	16.88	15.77 ± 0.9	0.185
0_N9	0	15.19		0.207
0_N13	0	16.38		0.191
45_N1	45	8.66	8.92 ± 1.2	1.401
45_N2	45	10.72		1.457
45_N8	45	8.20		1.514
90_N2	90	2.26	4.21 ± 1.8	1.665
90_N3	90	4.42		1.354
90_N7	90	5.96		1.525
90_N8	90	4.56	3.73 ± 1.6	0.201
90_N9	90	1.91		0.116
90_N11	90	4.95		0.193

$$\mathrm{DIF}_{\mathrm{CEB}} = \begin{cases} 1 & \dot{\varepsilon}_d \le \dot{\varepsilon}_s \\ \left(\frac{\dot{\varepsilon}_d}{\dot{\varepsilon}_s}\right)^{1.016\alpha} & \dot{\varepsilon}_s < \dot{\varepsilon}_d \le 30\,\mathrm{s}^{-1} \\ \gamma\left(\frac{\dot{\varepsilon}_d}{\dot{\varepsilon}_s}\right)^{0.33} & \dot{\varepsilon}_d > 30\,\mathrm{s}^{-1} \end{cases} \quad (11)$$

with $\gamma = 10^{(7.11\alpha-2.33)}$, $\alpha = 1/(10 + 6f_c/10)$ (f_c is the compressive strength in MPa) and $\dot{\varepsilon}_s = 3 \times 10^{-6}\,\mathrm{s}^{-1}$.

(b) the DIF formula proposed by Malvar and Crawford (1998) and based on the previous one:

$$\mathrm{DIF}_{\mathrm{Malvar\ \&\ Crawford}} = \begin{cases} 1 & \dot{\varepsilon}_d \le \dot{\varepsilon}_s \\ \left(\frac{\dot{\varepsilon}_d}{\dot{\varepsilon}_s}\right)^{\alpha} & \dot{\varepsilon}_s < \dot{\varepsilon}_d \le 1\,\mathrm{s}^{-1} \\ \gamma\left(\frac{\dot{\varepsilon}_d}{\dot{\varepsilon}_s}\right)^{0.33} & \dot{\varepsilon}_d > 1\,\mathrm{s}^{-1} \end{cases} \quad (12)$$

with $\gamma = 10^{(6\alpha-2)}$, $\alpha = 1/(1 + 8f_c/10)$ (f_c is the compressive strength in MPa) and $\dot{\varepsilon} = 1 \times 10^{-6}\,\mathrm{s}^{-1}$.

(c) or the DIF formula proposed by Zhou and Hao (2008) recommended for concrete-like materials, which is fitted from past experimental results

$$\mathrm{DIF}_{\mathrm{Zhou\ and\ Hao}} = \begin{cases} 1 & \dot{\varepsilon}_d \le 10^{-4}\,\mathrm{s}^{-1} \\ 2.06 + 0.26\log(\dot{\varepsilon}_d) & 10^{-4}\,\mathrm{s}^{-1} < \dot{\varepsilon}_d \le 1\,\mathrm{s}^{-1} \\ 2.06 + 2\log(\dot{\varepsilon}_d) & \dot{\varepsilon}_d > 1\,\mathrm{s}^{-1} \end{cases} \quad (13)$$

Figures 9 and 10 illustrate the increase of the DIF versus strain rate and stress rate, respectively. It is shown that at lower strain rates the strength increase is gradual above a certain strain rate, while this increase is drastic for higher strain rates. This transition seems to be present in the lower strength rocks and might be less marked for the higher strength rocks. This transition may be dependent on rock type and loading.

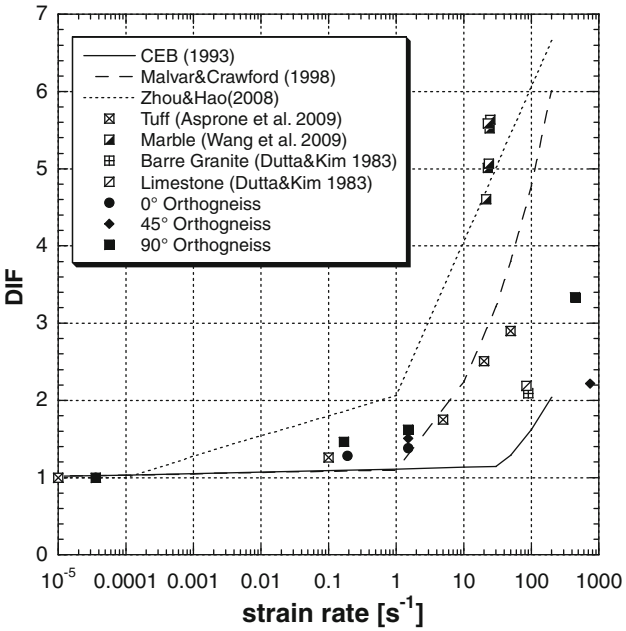

Fig. 9 DIF versus strain rate for different rocks

Figure 10 confirms that a more suitable formulation is necessary for rocks and that a wide experimental campaign on different families of rocks is needed. In fact Eqs. 11, 12 and 13 do not describe well the evolution of the DIF of the rock materials, often overestimating the dynamic strength or, in case of CEB formulation, strongly

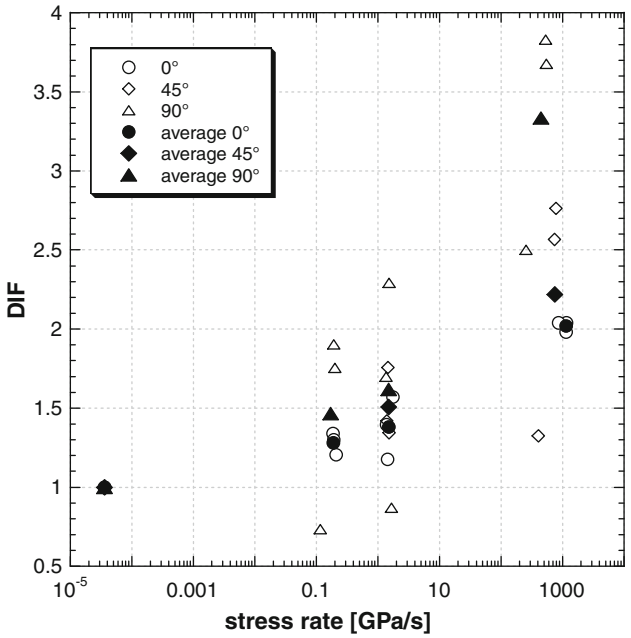

Fig. 10 DIF versus stress rate for the Orthogneiss at $\theta = 0°$, 45° and 90°

underestimating it (this can be explained considering that this formula has been developed for concrete and addressed to civil engineers for design).

Figure 10 shows the effect of the orientation on the dynamic tensile strength. It can be observed how the dispersion of the results is quite high in the case of $\theta = 45°$ and 90°. The tests at $\theta = 0°$ demonstrate instead a better reproducibility of the results.

6 Conclusions

Rock tensile strength is strain rate-dependent. It has been verified that also for the Orthogneiss this strength increases with the strain rate increasing within the wide strain rate range. The results show a non-linear relationships between strength and strain rates and the influence of the loading direction with respect to the schistosity of the rock examined.

The results presented in this paper show the capability of the JRC-SHTB in measuring the entire stress–strain curves of brittle materials like rocks, including the softening branch.

The results confirm that a more suitable formulation is necessary to describe DIF evolution in function of the strain rate for rocks. A large experimental campaign should be performed on different rock types and in a wide range of strain rates. The experimental techniques presented in this paper have demonstrated to be a proper tool for this purpose.

Acknowledgments The author would like to express his sincere gratitude to Matteo Dotta, Daniele Forni and Samuel Antonietti of the University of Applied Sciences of Southern Switzerland for their precious help in the analysis of the data and in the execution of the laboratory tests.

References

Albertini C, Montagnani M (1974) Testing techniques based on the split Hopkinson bar. In: Proceedings of the international conference on "the mechanical properties at high strain-rates", Oxford University, Institute of Physics Conference Series, no. 21, pp 22–32

Albertini C, Cadoni E, Labibes K (1996) Dynamic mechanical behaviour of large concrete specimen by means of a bundle Hopkinson bars. In: Proceedings of the 2nd international symposium on impact engineering, Chinese Mechanics Journal, Beijing, pp 214–219

Albertini C, Cadoni E, Labibes K (1997) Impact fracture process and mechanical properties of plain concrete by means of an Hopkinson bar bundle. J Phys III(7):915–920

Albertini C, Cadoni E, Labibes K (1999) Study of the mechanical properties of plain concrete under dynamic loading. Exp Mech 39:137–141

Asprone D, Cadoni E, Prota A, Manfredi G (2009) Dynamic behavior of a Mediterranean natural stone under tensile loading. Int J Rock Mech Min Sci 46:514–520

Barla G, Innaurato N (1973) Indirect tensile testing of anisotropic rocks. Rock Mech 5:215–230

Cadoni E, Labibes K, Solomos G, Albertini C (1997) Mechanical response in tension of plain concrete in a large range of strain-rates, Technical Note No. I.97.194, European Commission, Joint Research Centre

Cadoni E, Labibes K, Berra M, Giangrasso M, Albertini C (2000) High strain-rate tensile concrete behaviour. Mag Concr Res 52:365–370

Cadoni E, Labibes K, Berra M, Giangrasso M, Albertini C (2001a) Influence of the aggregate size on the strain-rate tensile behaviour of concrete. ACI Mater J 98:220–223

Cadoni E, Albertini C, Labibes K, Solomos G (2001b) Behaviour of plain concrete subjected to tensile loading at high strain-rate. In: Proceedings of the 4th international conference on fracture mechanics of concrete and concrete structures, vol 1, June 2001, ENS-Cachan, pp 341–348

Cadoni E, Labibes K, Albertini C, Berra M, Giangrasso M (2001c) Strain-rate effect on the tensile behaviour of concrete at different relative humidity levels. Mater Struct 34:21–26

Cadoni E, Solomos G, Albertini C (2009) Mechanical characterization of concrete in tension and compression at high strain-rate using a modified Hopkinson bar. Mag Concr Res 61:221–230

Comité Euro-International du Béton (1993) CEB-FIP Model Code 1990. Redwood Books, Trowbridge, Wiltshire, UK

Davies RM (1948) A critical study of the Hopkinson pressure bar. Phil Trans R Soc Lond Ser A 240:375–457

Dutta PK, Kim K (1983) High-strain-rate tensile behavior of sedimentary and igneous rocks at low temperatures. US Army Corps of Engineers, Cold Regions Research & Engineering Laboratory CRREL Report 93-16, p 17

Hillerborg A, Modeer M, Peterson PE (1976) Analysis of crack formation and crack growth in concrete by means of fracture mechanics and finite elements. Cem Concr Res 6:773–778

Klepaczko JR, Brara A (2001) Experimental method for dynamic tensile testing of concrete by spalling. Int J Impact Eng 25:387–409

Kolsky H (1949) An investigation of the mechanical properties of materials at very high rates of loading. Proc Phys Soc Sect B 62:676–700

Kubota S, Ogata Y, Wada Y, Simangunsong G, Shimada H, Matsui K (2008) Estimation of dynamic tensile strength of sandstone. Int J Rock Mech Min Sci 45:397–406

Malvar LJ, Crawford JE (1998) Dynamic increase factors for concrete. Twenty-eighth DDESB seminar, Orlando

Reinhardt HW, Körmeling HA, Zielinski AJ (1986) The split Hopkinson bar, a versatile tool for the impact testing of concrete. Mater Struct 19:55–63

Schuler H, Mayrhofer C, Thoma K (2006) Spall experiments for the measurement of the tensile strength and fracture energy of concrete at high strain rates. Int J Impact Eng 32:1635–1650

Tedesco JW, Ross CA, Kuennen ST (1993) Experimental and numerical analysis of high strain rate splitting tensile tests. ACI Mater J 90:162–169

Wang QZ, Li W, Xie HP (2009) Dynamic split tensile test of Flattened Brazilian Disc of rock with SHPB setup. Mech Mater 41:252–260

Zhou XQ, Hao H (2008) Mesoscale modelling of concrete tensile failure mechanism at high strain rates. Comput Struct 86:2013–2026

Zielinski AJ (1982) Fracture of concrete and mortar under uniaxial impact tensile loading. Doctoral Thesis, Delft University of Technology, The Netherlands